frontiers | Frontiers in Physics

TYPE Original Research
PUBLISHED 02 August 2024
DOI 10.3389/fphy.2024.1437341

Check for updates

OPEN ACCESS

EDITED BY
Xuzhen Zhu,
Beijing University of Posts and Telecommunications (BUPT), China

REVIEWED BY
Ruiqi Li,
Beijing University of Chemical Technology, China
Peican Zhu,
Northwestern Polytechnical University, China

*CORRESPONDENCE
Jiajun Xian,
xianjiajun22@gmail.com

RECEIVED 23 May 2024
ACCEPTED 02 July 2024
PUBLISHED 02 August 2024

CITATION
Zhang W, Ye Y, Li Z, Xian J, Wang T, Liu D, Hu D and Liu M (2024), The coupled awareness-epidemic dynamics with individualized self-initiated awareness in multiplex networks. *Front. Phys.* 12:1437341. doi: 10.3389/fphy.2024.1437341

COPYRIGHT
© 2024 Zhang, Ye, Li, Xian, Wang, Liu, Hu and Liu. This is an open-access article distributed under the terms of the Creative Commons Attribution License (CC BY). The use, distribution or reproduction in other forums is permitted, provided the original author(s) and the copyright owner(s) are credited and that the original publication in this journal is cited, in accordance with accepted academic practice. No use, distribution or reproduction is permitted which does not comply with these terms.

The coupled awareness-epidemic dynamics with individualized self-initiated awareness in multiplex networks

Wei Zhang[1], Yixuan Ye[1], Zongyi Li[1], Jiajun Xian[2,3]*, Teng Wang[1], Dandan Liu[4], Die Hu[5] and Ming Liu[2,3]

[1]Department of Computer Science, Shantou University, Shantou, China, [2]Yangtze Delta Region Institute (Quzhou), University of Electronic Science and Technology of China, Quzhou, Zhejiang, China, [3]Quzhou People's Hospital, Quzhou Affiliated Hospital of Wenzhou Medical University, Quzhou, Zhejiang, China, [4]Department of Automation, School of Electrical Engineering, Yancheng Institute of Technology, Yancheng, China, [5]Environment Design Department, Chengdu University, Chengdu, China

The outbreak of an epidemic often stimulates the generation of public awareness about epidemic prevention. This heightened awareness encourages individuals to take proactive protective measures, thereby curbing the transmission of the epidemic. Previous research commonly adopts an assumption that each individual has the same probability of awakening self-protection awareness after infection. However, in the real-world process, different individuals may generate varying awareness responses due to the differences in the amount of information received. Therefore, in this study, we first propose a coupled awareness-epidemic spreading model, where the self-initiated awareness of each individual can be influenced by the number of aware neighbors. Subsequently, we develop a Micro Markov Chain Approach to analyze the proposed model and explore the effects of different dynamic and structural parameters on the coupled dynamics. Findings indicate that individual awareness awakening can effectively promote awareness diffusion within the proposed coupled dynamics and inhibit epidemic transmission. Moreover, the influence of awareness diffusion on epidemic transmission exhibits a metacritical point, from which the epidemic threshold increases with the increase in the awareness diffusion probability. The research findings also suggest that the increase in the average degree of virtual-contact networks can reduce the value of the metacritical point, while the change in the average degree of the physical-contact networks does not affect the metacritical point. Finally, we conduct extensive experiments on four real networks and obtain results consistent with the above conclusions. The systematic research findings of this study provide new insights for exploring the interaction between individual awareness and epidemic transmission in the real world.

KEYWORDS

multiplex networks, coupled awareness-epidemic dynamics, self-initiated awareness, metacritical point, complex networks

1 Introduction

The spread of infectious diseases poses a significant threat to human health and can lead to substantial economic losses [1]. Throughout history, human society has repeatedly suffered devastating impacts from infectious diseases. For example, in the 16th and 17th centuries, the rampant smallpox virus led to a sharp decline in the population of indigenous peoples in the Americas. The outbreak of novel coronavirus pneumonia (COVID-19) in 2019 has caused nearly seven million deaths worldwide [2–4]. It is worth noting that the large-scale outbreak of an epidemic often effectively stimulates individuals to develop self-initiated awareness, which can effectively curb the spread of the epidemic [5–9]. For example, after the outbreak of the COVID-19 pandemic, information related to it started diffusing on social networks or community networks, thereby sparking the development of individual awareness about epidemic prevention [10, 11]. After developing self-initiated awareness, individuals will actively take a series of self-protective measures to reduce the risk of infection, such as wearing masks, frequent hand-washing, reducing outdoor activities, maintaining social distancing, and more [12]. These self-protective measures can effectively interrupt the transmission pathways of the virus, thereby suppressing further transmission of the disease [13–17]. Therefore, how to model and analyze the coupled awareness-epidemic dynamics has long been a subject of significant interest among scholars from various fields.

In real life, individuals can not only have physical contact with others, such as shaking hands and sharing meals, which promote the spread of diseases but also communicate with others to receive disease-related information and generate awareness of self-protection [18–22]. Therefore, in recent years, scholars typically adopt a two-layer multiplex network structure to establish the coupled awareness-epidemic dynamics in their research, aiming to explore the interaction between awareness diffusion and epidemic transmission in the real world [23–27]. In the two-layer multiplex network structure, the first layer is the physical-contact network, where nodes represent individuals in the real world, and edges represent physical contact relationships between individuals; the second layer (virtual contact) is the network with the same nodes as the physical-contact network, while edges represent information interaction between individuals [28–31]. In 2013, Granell et al. proposed a coupled awareness-epidemic dynamics model with the multiplex network structure to investigate the real-world coupled awareness-epidemic dynamics. They identified the presence of a metacritical point for awareness diffusion rate, and when the awareness diffusion rate is larger than this point, the epidemic threshold will increase with it [32]. Subsequently, scholars have proposed several improved models from different perspectives to consider the effects of various real-world factors on the coupled awareness-epidemic dynamics. For instance, Granell et al. further integrates mass media into the awareness diffusion process, elucidating that the metacritical point for epidemic outbreaks vanishes under the influence of mass media [33]. Chen et al. introduced a resource-epidemic coevolution model on a multiplex network and discovered an optimal heterogeneity of self-awareness at which the disease can be suppressed to the greatest extent [34]. Wu et al. introduce a two-layer network where the inter-layer coupling is induced by the movement of traveler individuals between layers, and they find that travelers' hopping preference for different layers can lead to non-monotonic changes in the epidemic threshold and spreading coverage [35]. Furthermore, many scholars have delved into the effects of the spatio-temporal characteristics of networks on epidemic spreading. Liu et al. proposed a spatio-temporal network model based on co-location interactions using massive cellphone data. They reveals that universal laws underlying spatio-temporal contact patterns among residents is essential for epidemic spreading [36]. Furthermore, Li et al. introduced a temporal multiplex network consisting of a static information spreading network and a temporal physical contact network with a layer-preference walk. They found that the epidemic threshold decreases with the decrease of the effective information spreading rate and the increase of the layer [37].

As mentioned above, scholars have made significant progress in the study of coupled awareness-epidemic dynamics. However, there is limited research that incorporates individualized self-initiated awareness into the coupled awareness-epidemic dynamics. In the real world coupled awareness-epidemic spreading, different individuals generate varying awareness responses due to the differences in the amount of information received from their neighbors. Hence, research on the coupled awareness-epidemic dynamics that takes into account individualized self-initiated awareness holds significant importance. In light of this, this study first proposes a coupled awareness-epidemic dynamics model that incorporates individualized self-initiated awareness, where the probability of infected individuals developing self-initiated awareness is influenced by the number of their aware neighbors. Subsequently, we develop the Microscopic Markov Chains Approach to theoretically analyze the aforementioned model and investigate the effects of crucial dynamics and structural parameters on the coupled awareness-epidemic dynamics.

The paper is structured as follows: Section 2 provides a detailed description of the coupled awareness-epidemic dynamics with individualized self-initiated awareness. In Section 3, we introduce the Micro Markov Chain Approach to analyze the previous model, and derive the stationary spread range and transmission threshold of the epidemic. In Section 4, we explore the effects of different dynamics and structural parameters on the coupled awareness-epidemic dynamics. Finally, Section 5 summarizes the entire work and outlines potential avenues for further study.

2 Model description

In the study, we consider the coupled awareness-epidemic dynamics on top of a two-layer multiplex networks as shown in Figure 1. The nodes of the two network layers are one-to-one correspondence, but the connectivity between them is different. Awareness of the epidemic diffuses on the second layer of the multiplex network (namely, the virtual-contact layer), and the epidemic takes place on the first layer (namely, the physical-contact network).

In the virtual-contact layer, an unaware-aware-unaware (UAU) model is adopted to depict the diffusion of epidemic awareness. Unaware (U) nodes have no epidemic awareness and will take no precautions against the epidemic, while aware (A) nodes know about the epidemic and will take certain preventive measures. The

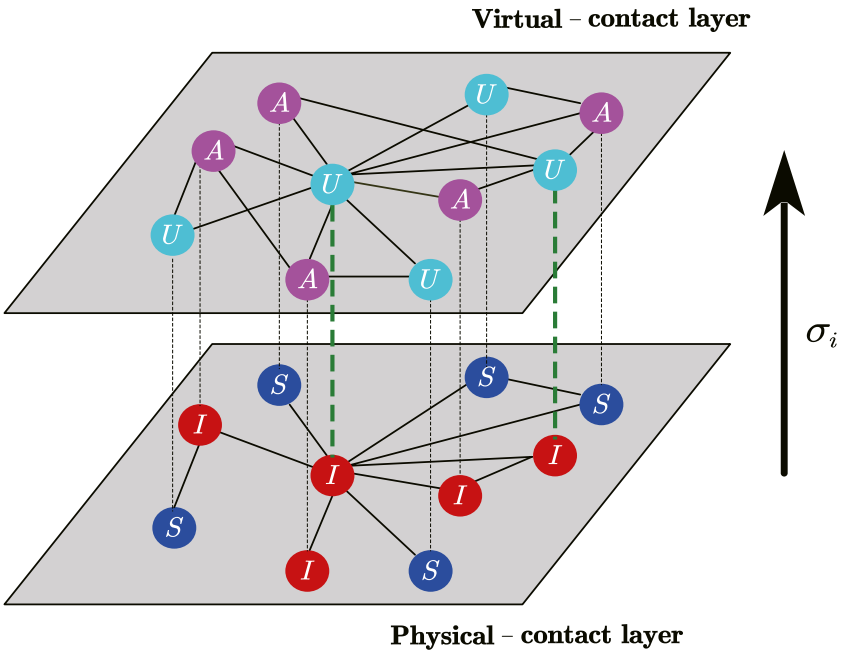

FIGURE 1
(Color online) A schematic illustration showcasing the coupled awareness-epidemic dynamics with individualized self-initiated awareness in multiplex networks. The first layer (physical-contact network) employs a susceptible-infected-susceptible (SIS) model to delineate the transmission of the epidemic. Within this layer, susceptible (S) nodes can be infected by their infected (I) neighbors. The second layer corresponds to the virtual-contact network, sharing identical nodes with the physical-contact network. In this layer, an unaware-aware-unaware (UAU) model captures the diffusion of epidemic awareness. Nodes in the unaware (U) state lack epidemic awareness and consequently take no preventive measures. Conversely, the aware (A) nodes possess knowledge about the epidemic and implement specific precautionary measures. Additionally, when a node in the unaware state becomes infected, it has a probability of σ_i to develop epidemic awareness autonomously.

diffusion of epidemic awareness occurs from the A-state node to the U-state node with a probability of λ, while the A-state node can revert to the U-state due to loss of awareness with a probability of δ. Besides, the moment when the U-state node is infected with the disease, it will develop a self-initiated awareness with the probability given by Eq. 1:

$$\sigma_i(t) = 1 - (1 - \sigma_0)^{\eta_A(t)+1} \tag{1}$$

where $\eta_A(t)$ is the count of neighbors in A-state of node i.

In physical-contact layer, a susceptible-infected-susceptible (SIS) model is adopted to describe the epidemic-transmitting process. The susceptible (S) node, both with and without epidemic awareness, can become infected by its infected (I) neighbor with the certain probability of β, and $\beta^A = \gamma\beta$, respectively, where $0 \le \gamma \le 1$ is an attenuation factor reflecting the influence of preventive measures taken by A-state nodes. Additionally, the likelihood of an infected node recovering spontaneously is represented by μ.

3 Theoretical analysis

3.1 Microscopic markov chain approach

We will provide an analytical derivation based on the Microscopic Markov Chain Approach (MMCA) for our model in this section. Denote $A = (a_{ij})_N$ and $B = (b_{ij})_N$ as the adjacency matrixes for the virtual-contact layer and physical-contact layer, respectively, where N represents the number of nodes. Taking both the virtual-contact layer and physical-contact layer into consideration, nodes within our model have four possible states, i.e., unaware-susceptible (US), aware-susceptible (AS), unaware-infected (UI), and aware-infected (AI). Let $P_i^{US}(t)$, $P_i^{AS}(t)$, $P_i^{UI}(t)$, $P_i^{AI}(t)$ denote the probability of node i being in US-state, AS-state, UI-state, AI-state at time t, respectively. The probability of node i being in A-state, U-state, I-state, and S-state can be calculated as $P_i^A = P_i^{AS}(t) + P_i^{AI}(t)$, $P_i^U = P_i^{US}(t) + P_i^{UI}(t)$, $P_i^I = P_i^{AI}(t) + P_i^{UI}(t)$, and $P_i^S = P_i^{US}(t) + P_i^{IS}(t)$, respectively. Besides, the probability of the U-state node i not being informed by any neighbor at time t can be given by Eq. 2.

$$\theta_i(t) = \prod_j \left[1 - a_{ij} P_j^A(t)\lambda\right] \tag{2}$$

The probabilities of node i being in the unaware-susceptible (US) state and the aware-susceptible (AS) state, and not being infected at time t, are given by Eqs 3 and 4, respectively.

$$q_i^U(t) = \prod_j \left[1 - b_{ij} P_j^I(t)\beta^U\right] \tag{3}$$

$$q_i^A(t) = \prod_j \left[1 - b_{ij} P_j^I(t)\beta^A\right] \tag{4}$$

Figure 2 shows the transition probability trees for the four possible states of nodes in our model. The dynamics governing $P_i^{UI}(t)$, $P_i^{US}(t)$, $P_i^{AS}(t)$, and $P_i^{AI}(t)$ are encapsulated in Eqs 5–8, respectively.

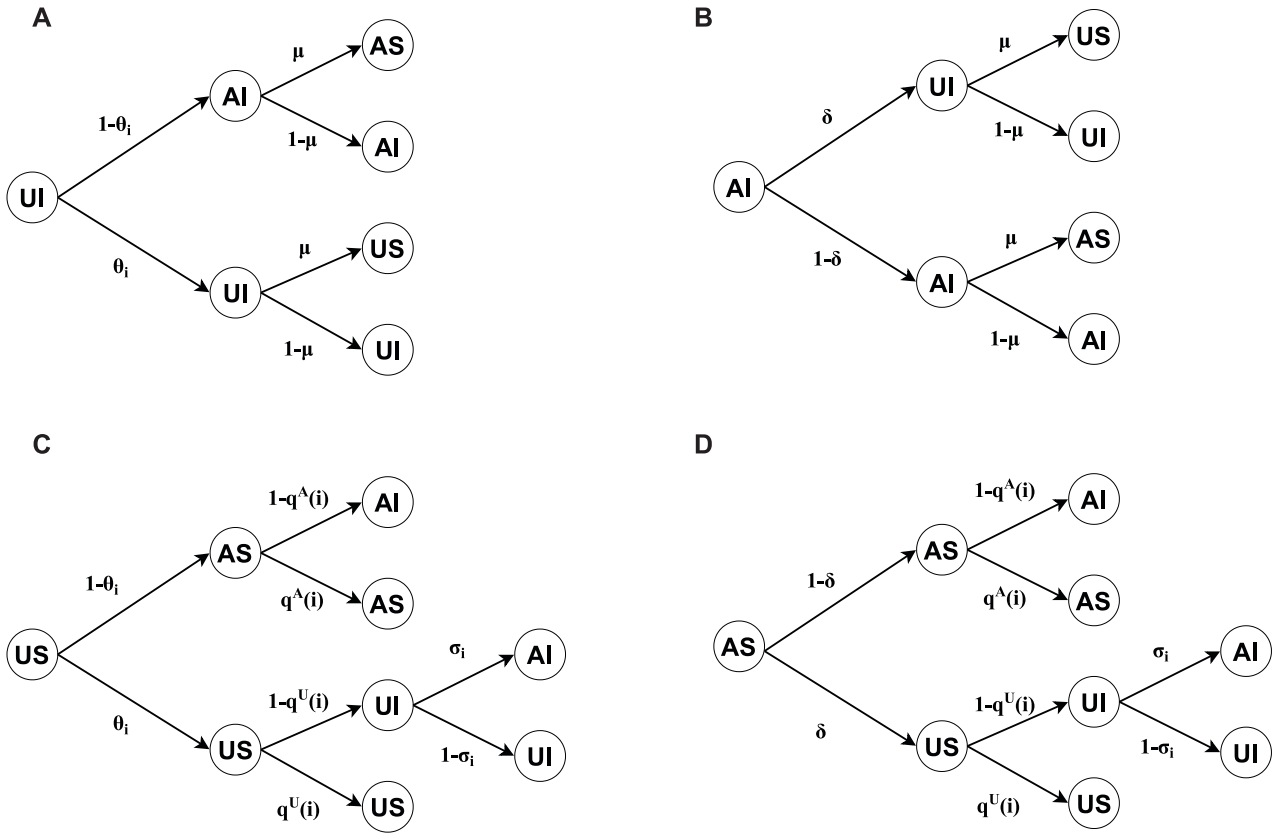

FIGURE 2
Transition probability trees are illustrated for four distinct node states: **(A)** unaware-infected (UI), **(B)** aware-infected (AI), **(C)** unaware-susceptible (US), and **(D)** aware-susceptible (AS). The tree roots denote the state of each node at time t, while their possible states at time $t+1$ are denoted by the leaves.

$$\begin{aligned} P_i^{\mathrm{UI}}(t+1) = {} & P_i^{\mathrm{UI}}(t)\theta_i(t)(1-\mu) + P_i^{\mathrm{AI}}(t)\delta(1-\mu) \\ & + P_i^{\mathrm{US}}(t)\theta_i(t)\left[1-q_i^{\mathrm{U}}(t)\right]\left[1-\sigma_i(t)\right] \\ & + P_i^{\mathrm{AS}}(t)\delta\left[1-q_i^{\mathrm{U}}(t)\right]\left[1-\sigma_i(t)\right] \end{aligned} \tag{5}$$

$$\begin{aligned} P_i^{\mathrm{US}}(t+1) = {} & P_i^{\mathrm{UI}}(t)\theta_i(t)\mu + P_i^{\mathrm{AI}}(t)\delta\mu \\ & + P_i^{\mathrm{US}}(t)\theta_i(t)q_i^{\mathrm{U}}(t) + P_i^{\mathrm{AS}}(t)\delta q_i^{\mathrm{U}}(t) \end{aligned} \tag{6}$$

$$\begin{aligned} P_i^{\mathrm{AS}}(t+1) = {} & P_i^{\mathrm{UI}}(t)\left[1-\theta_i(t)\right]\mu + P_i^{\mathrm{AI}}(t)(1-\delta)\mu \\ & + P_i^{\mathrm{US}}(t)\left[1-\theta_i(t)\right]q_i^{\mathrm{A}} + P_i^{\mathrm{AS}}(t)(1-\delta)q_i^{\mathrm{A}} \end{aligned} \tag{7}$$

$$\begin{aligned} P_i^{\mathrm{AI}}(t+1) = {} & P_i^{\mathrm{UI}}(t)\left[1-\theta_i(t)\right](1-\mu) + P_i^{\mathrm{AI}}(t)(1-\delta)(1-\mu) \\ & + P_i^{\mathrm{US}}(t)\left\{\left[1-\theta_i(t)\right]\left[1-q_i^{\mathrm{A}}(t)\right] + \theta_i(t)\left[1-q_i^{\mathrm{U}}(t)\right]\sigma_i(t)\right\} \\ & + P_i^{\mathrm{AS}}(t)\left\{\delta\left[1-q_i^{\mathrm{U}}(t)\right]\sigma_i(t) + (1-\delta)\left[1-q_i^{\mathrm{A}}(t)\right]\right\} \end{aligned} \tag{8}$$

3.2 Threshold analysis

The epidemic threshold is given by the parameter ρ^{I}, i.e., the fraction of I-state nodes in the system, and is calculated as shown in Eq. 9.

$$\rho^{\mathrm{I}} = \frac{1}{N}\sum_{i=1}^{N} P_i^{\mathrm{I}} = \frac{1}{N}\sum_{i=1}^{N}\left(P_i^{\mathrm{UI}} + P_i^{\mathrm{AI}}\right) \tag{9}$$

In the steady state, by summing Eqs 5, 8, we acquire

$$\begin{aligned} P_i^{\mathrm{I}} = {} & P_i^{\mathrm{I}}(1-\mu) + P_i^{\mathrm{US}}\left[\theta_i\left(1-q_i^{\mathrm{U}}\right) + (1-\theta_i)\left(1-q_i^{\mathrm{A}}\right)\right] \\ & + P_i^{\mathrm{AS}}\left[\delta\left(1-q_i^{\mathrm{U}}\right) + (1-\delta)\left(1-q_i^{\mathrm{A}}\right)\right]. \end{aligned} \tag{10}$$

Near the epidemic threshold, the fraction of I-state nodes is close to zero, i.e., $P_i^{\mathrm{I}} = \varepsilon_i \ll 1$. Accordingly, q_i^{U} and q_i^{A} can be approximately calculated as

$$q_i^{\mathrm{U}} \approx 1 - \beta^{\mathrm{U}}\sum_j b_{ji}\varepsilon_j = 1 - \omega_i, \tag{11}$$

and

$$q_i^{\mathrm{A}} \approx 1 - \gamma\beta^{\mathrm{U}}\sum_j b_{ji}\varepsilon_j = 1 - \gamma\omega_i, \tag{12}$$

respectively, where ω_i is given by Eq. 13:

$$\omega_i = \beta^{\mathrm{U}}\sum_j b_{ji}\varepsilon_j. \tag{13}$$

Substituting Eqs 11, 12 into Eq. 10 leads to

$$\begin{aligned} \varepsilon_i &= \varepsilon_i(1-\mu) + P_i^{\mathrm{US}}\left[\theta_i\omega_i + (1-\theta_i)\gamma\omega_i\right] \\ &\quad + P_i^{\mathrm{AS}}\left[\delta\omega_i + (1-\delta)\gamma\omega_i\right] \\ &= \varepsilon_i(1-\mu) + \left(P_i^{\mathrm{U}}\theta_i + P_i^{\mathrm{A}}\delta\right)\omega_i \\ &\quad + \left[P_i^{\mathrm{U}}(1-\theta_i) + P_i^{\mathrm{A}}(1-\delta)\right]\gamma\omega_i. \end{aligned} \tag{14}$$

Since $\varepsilon_i \ll 1$ in the stationary state, we should have $P_i^{US} = P_i^U - P_i^{UI} \approx P_i^U$ and $P_i^{AS} = P_i^A - P_i^{AI} \approx P_i^A$. Thus, removing $O(\varepsilon_i)$ terms in the stationary state of Eqs 6, 7 we get

$$P_i^U = P_i^U\theta_i + P_i^A\delta \tag{15}$$

and

$$P_i^A = P_i^U(1-\theta_i) + P_i^A(1-\delta). \tag{16}$$

Then, substituting Eqs 15, 16 into Eq. 14 leads to Eq. 17:

$$\begin{aligned}\varepsilon_i &= \varepsilon_i(1-\mu) + P_i^U\omega_i + P_i^A\gamma\omega_i \\ &= \varepsilon_i(1-\mu) + (P_i^U + P_i^A\gamma)\beta^U\sum_j b_{ji}\varepsilon_j,\end{aligned} \tag{17}$$

which can be written as

$$\sum_j\left[\beta^U\left[1+(\gamma-1)P_i^A\right]b_{ji} - \mu\delta_{ij}\right]\varepsilon_j = 0, \tag{18}$$

where δ_{ij} are the elements of the identity matrix. Defining matrix H with elements as given by Eq. 19:

$$h_{ji} = (P_i^U + \gamma P_i^A)b_{ji} = \left[1+(\gamma-1)P_i^A\right]b_{ji}, \tag{19}$$

the nontrivial solutions of Eq. 18 are eigenvectors of H, whose largest real eigenvalues are equal to the epidemic threshold

$$\beta_c = \frac{\mu}{\Lambda_{max}(H)}. \tag{20}$$

Equation 20 provides a quantitative representation indicating that the epidemic threshold is dependent on the spreading dynamics on both network layers.

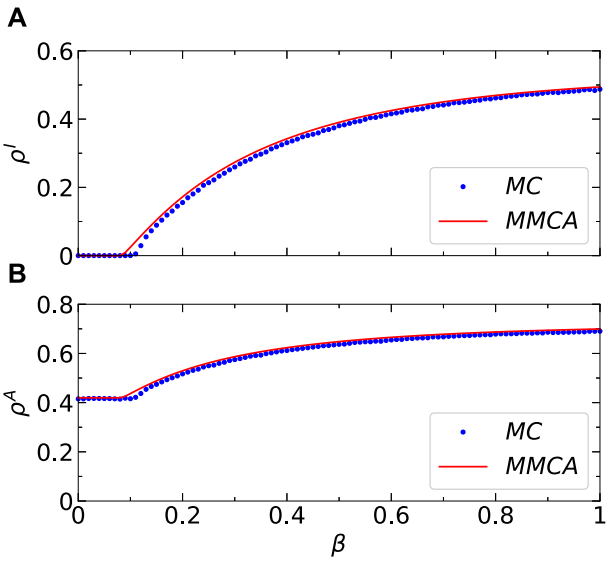

FIGURE 3
(Color online) Results comparisons between the Microscopic Markov Chains Approach (MMCA) and Monte Carlo (MC) simulations regarding the stationary fractions. **(A)** Comparisons between the stationary I-state individuals' fraction ρ^I obtained by MC simulations (dotted line) and the MMCA (solid line). **(B)** Comparisons between the stationary A-state individuals' fraction ρ^A obtained by Monte Carlo simulations (dotted line) and the MMCA (solid line). All the numerical simulations are performed on top of multiplex network G^0 and Additional parameters include $\mu = 0.5$ and $\gamma = 0$ in the physical-contact layer, $\lambda = 0.15$, $\sigma_0 = 0.5$, and $\delta = 0.6$ in the virtual-contact layer.

4 Simulation results

In this section, we explore the effects of various dynamics and structural parameters on the proposed coupled awareness-epidemic dynamics. In reality, the behavior of the same individual on the virtual-contact network and the physical-contact network may not be consistent. For example, individuals who appear active on the virtual-contact networks may have rare physical contact with others. To imitate the variability in individual behavior between the virtual-contact layer and the physical-contact layer, we employ three multiplex networks with varying inter-layer degree correlation r_s, namely, G^{-1}, G^0, and G^1, whose r_s are set to −1, 0, and 1, respectively. The physical-contact layers of the three multiplex networks are all sale-free networks with the number of nodes $N = 1000$, the average degree $K_A = 5$, and the degree exponent $\varepsilon = 5$. In addition, the virtual-contact layers are scale-free networks, sharing identical node counts and degree exponents with the physical-contact layers, but with the average degree $K_B = 10$. The setting of $K_A > K_B$ on the three multiplex networks is intended to imitate the real-world phenomenon where the density of virtual-contact networks is typically larger than that of physical-contact networks. We obtain the numerical simulation results presented in this section by averaging the outcomes of over 1,000 independent simulation experiments conducted on the aforementioned multiplex networks. Furthermore, we consistently set the initial infected nodes proportion in the epidemic transmission process at 0.2.

Firstly, we assess the efficacy of the MMCA method in describing the coupled awareness-epidemic dynamics proposed in this study on a group of multiplex networks. Figure 3 compares the dynamicsal results of the MMCA method and Monte Carlo (MC) simulation regarding ρ^I and ρ^A as a function of β on network G^0, which is a two-layer network with inter-layer degree correlation $r_s = 0$. In addition, Figure 4 shows the comparison results of ρ^I as a function of β and λ on three multiplex networks (that is, G^{-1}, G^0 and G^1) with distinct inter-layer degree correlations. It can be observed that the results obtained by the MMCA method have a good consistency with MC simulation in both Figures 3, 4, which verifies the accuracy and suitability of the MMCA method in solving the coupled awareness-epidemic spreading dynamics we proposed in this study. Hereinafter, we study the coupled dynamics proposed by the MMCA method.

Secondly, we conducted an analysis of how two significant dynamics parameters influence the stationary states of the proposedawareness-epidemic dynamics, namely, the basic self-initiated awareness probability σ_0 and infection attenuation factor γ, where σ_0 is the basic self-initiated awareness probability and the parameter γ governs the infection probability among aware individuals. Figures 5A–C illustrate the change of stationary I-state individuals fraction ρ^I with respect to the infection probability β on the multiplex networks G^{-1}, G^0, and G^1, respectively, when different values of σ_0 are considered. Observing the results, it can be concluded that when the value of σ_0 is non-zero, indicating that individuals on the networks

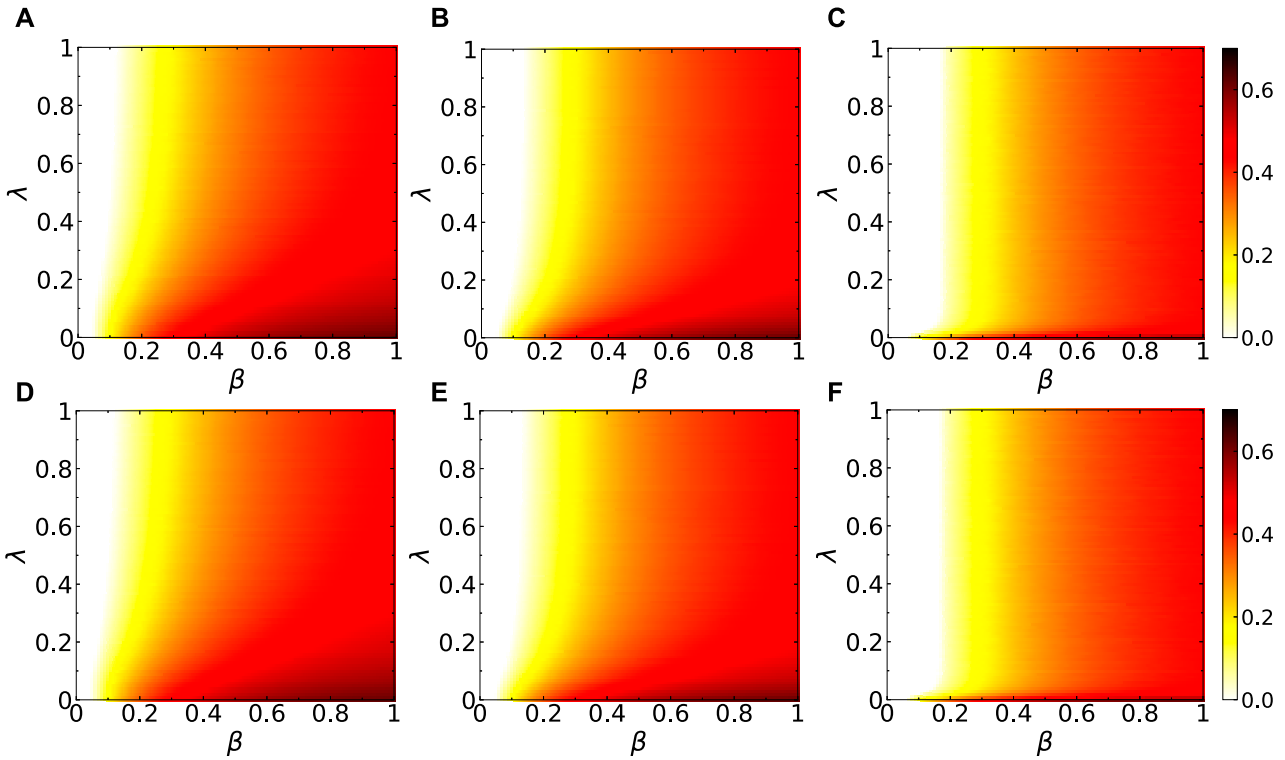

FIGURE 4
(Color online) Results comparisons of the full phase diagrams (λ-β) of ρ^{I} obtained by Microscopic Markov Chains Approach (MMCA) and Monte Carlo (MC) simulations. Top: the corresponding results of MMCA performed on top of multiplex network **(A)** G^{-1}, **(B)** G^{0}, and **(C)** G^{1}. Bottom: the corresponding results of MC simulations performed on top of multiplex network **(D)** G^{-1}, **(E)** G^{0}, and **(F)** G^{1}.The Additional parameters include $\mu = 0.5$ and $\gamma = 0$ in the physical-contact layer, $\lambda = 0.15$, $\sigma_0 = 0.5$, and $\delta = 0.6$ in the virtual-contact layer.

spontaneously generate self-initiated awareness, the stationary fraction of I-state individuals will be decreased on all the networks studied. It indicates that individual self-initiated awareness can suppress the process of epidemic transmission within the employed networks effectively. Figures 5D–F depict how the stationary A-state individuals fraction, denoted as ρ^{A}, varies in response to the infection probability β when considering different values of σ_0 on the multiplex networks G^{-1}, G^{0}, and G^{1}, respectively. Conclusions drawn from the results suggest that in the presence of a non-zero σ_0, ρ^{A} exhibits an increase across all the networks studied. Besides, with an increase in the σ_0 value, there is a corresponding rise in the value of ρ^{A}. Moreover, Figures 6A–C show the variation of ρ^{I} with respect to β on the multiplex networks G^{-1}, G^{0}, and G^{1}, respectively, when different values are set to γ. Upon scrutinizing the findings presented in the figures, it can be deduced that a decrease in the γ value results in a diminishment of ρ^{I} across all the networks studied. This is because in the proposed model, it is established that $\beta^{\mathrm{A}} = \gamma\beta^{\mathrm{U}}$. As the γ decreases, β^{A} also decreases, indicating a lower infection probability among aware individuals. Therefore, under the same dynamics conditions, the stationary fraction of ρ^{I} decreases with the decrease in γ.

Thirdly, we further analyzed the effects of three critical dynamics parameters on the epidemic threshold, namely, the infection attenuation factor γ, the diffusion probability of awareness λ, and the forgetting probability of aware individuals δ. Figure 7 portrays the variation of the epidemic threshold β_c concerning the infection attenuation factor γ on the multiplex networks with different inter-layer degree correlations. Analyzing the results from the figure, it can be inferred that a reduction in γ leads to an enhanced inhibitory impact of awareness on the epidemic, consequently yielding a larger value for β_c. Moreover, in network G^{1}, the β_c increases the fastest as γ decreases. This indicates that when there is a positive inter-layer degree correlation within the networks, the highly connected nodes in the awareness-spreading layer are more likely to become aware, which can enhance the epidemic threshold. Figures 8A–C depict how the epidemic threshold β_c varies concerning the awareness diffusion probability λ across the multiplex networks G^{-1}, G^{0}, and G^{1}, respectively, while considering distinct values for the awareness forgetting probability. As depicted in the figures, on all the networks studied, there is a metacritical point for the effects of awareness diffusion on epidemic transmission. Only when the awareness diffusion probability λ exceeds this metacritical point λ_c, does the epidemic threshold increase with the increasing awareness diffusion probability. Additionally, a decrease in the awareness of forgetting probability δ leads to an increase in β_c and a decrease in λ_c. This is because a smaller forgetting probability δ results in more persistent and widespread diffusion, which promotes the increase of epidemic threshold β_c and the decrease of the metacritical point λ_c that corresponds to it.

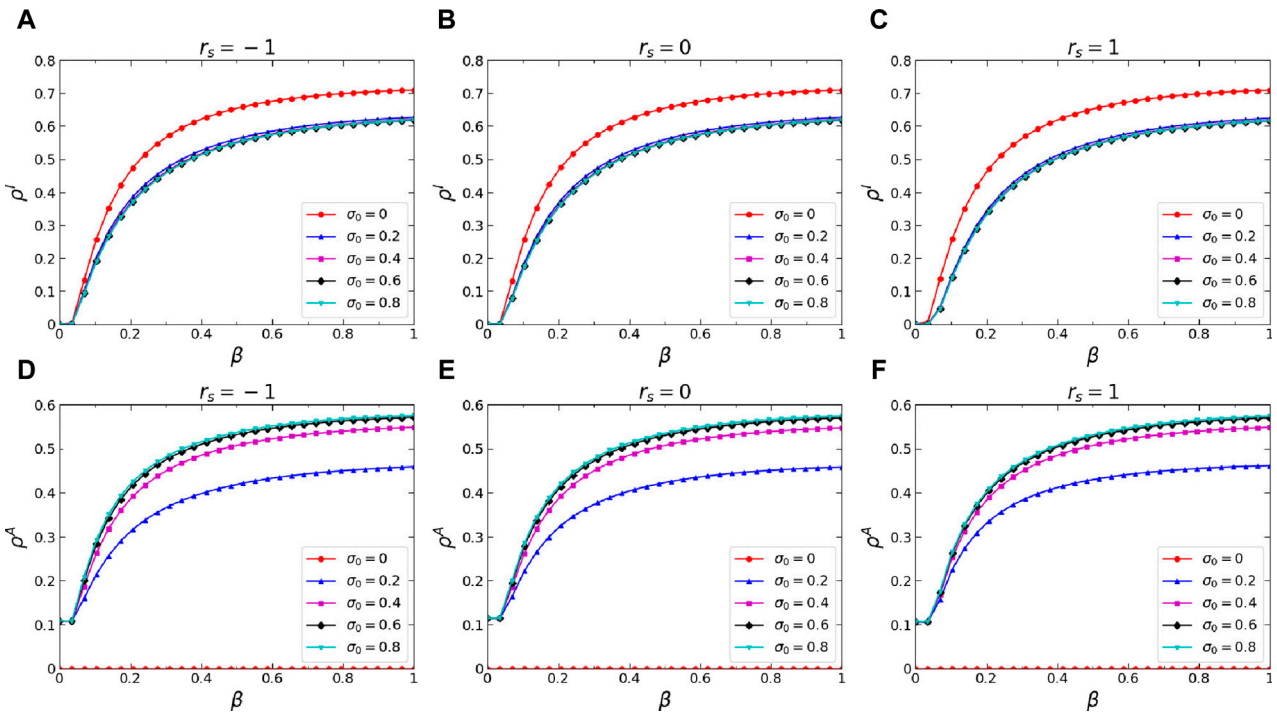

FIGURE 5
(Color online) Effects of the basic self-initiated awareness probability σ_0 on the stationary I-state individuals fraction ρ^I and stationary A-state individuals fraction ρ^A. Specifically, the stationary infeted individuals fraction ρ^I versus infection probability β when **(A)** $r_s = -1$, **(B)** $r_s = 0$, and **(C)** $r_s = 1$. The stationary aware individuals fraction ρ^A versus infection probability β when **(D)** $r_s = -1$, **(E)** $r_s = 0$, and **(F)** $r_s = 1$. The results when $\sigma_0 = 0$, $\sigma_0 = 0.2$, $\sigma_0 = 0.4$, $\sigma_0 = 0.6$, and $\sigma_0 = 0.8$ are denoted by red circle lines, blue trilateral lines, magenta square lines, black rhombus lines, and cyan inverted-triangle lines, respectively. Additional parameters include $\mu = 0.5$ and $\gamma = 0$ in the physical-contact layer, $\delta = 0.6$ and $\lambda = 0.15$ in the virtual-contact layer.

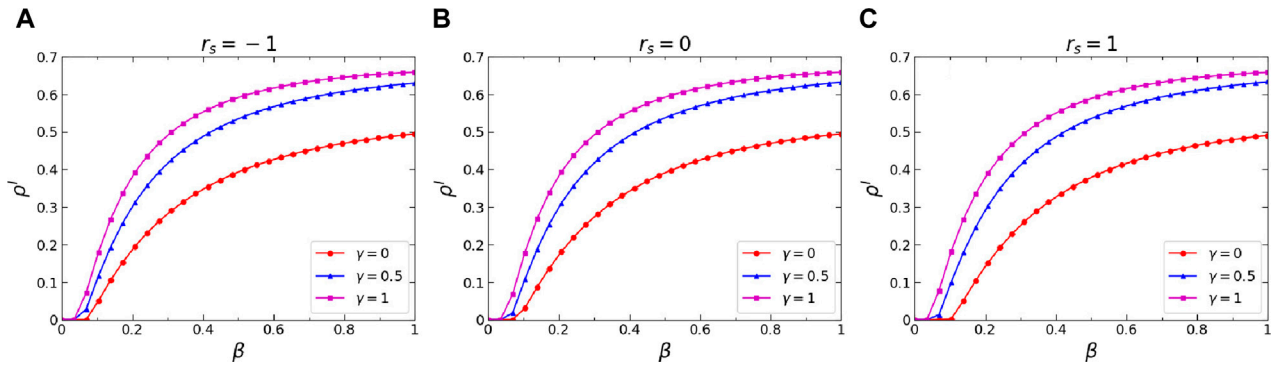

FIGURE 6
(Color online) Effects of the infection attenuation factor γ on the stationary I-state individuals fraction ρ^I. Specifically, the stationary I-state individuals fraction ρ^I versus infection probability β when **(A)** $r_s = -1$, **(B)** $r_s = 0$, and **(C)** $r_s = 1$. The outcomes corresponding to $\gamma = 0$, $\gamma = 0.5$, and $\gamma = 1$ are represented by red circular lines, blue triangular lines, and magenta square lines, respectively. Additional parameters include $\mu = 0.5$ in the physical-contact layer, $\lambda = 0.15$, $\sigma_0 = 0.5$, and $\delta = 0.6$ in the virtual-contact layer.

Finally, we investigate the effects of the average degree K_A and K_B of the virtual-contact layer and the physical-contact layer on the epidemic threshold β_c. In order to explore the role of K_A in the epidemic threshold, we construct three multiplex networks G^{K_A-5}, G^{K_A-10}, and G^{K_A-60} by randomly adding edges in virtual-contact network of G^1. The values of K_A in these networks are set to 5, 10, and 60, respectively, while keeping $K_B = 5$ constant. Figures 9A–C illustrate the changes of β_c concerning the awareness diffusion probability λ on three multiplex networks under different combinations of awareness forgetting probability δ and infected individual recovery probability μ. Comparing the results from the figures, it can be concluded that on all the networks studied, an increase in K_A not only leads to an increase in β_c but also causes a decrease in the metacritical point λ_c that corresponds to it. This

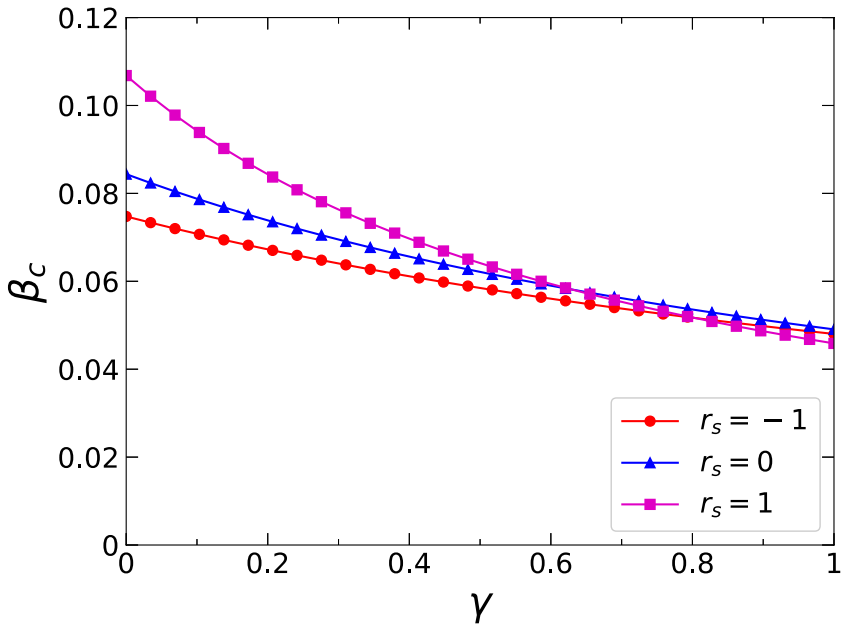

FIGURE 7
(Color online) Effects of the inter-layer degree correlations r_s on the epidemic threshold β_c. Specifically, the epidemic threshold β_c versus infection attenuation factor γ when $r_s = -1$, $r_s = 0$, and $r_s = 1$ are denoted by red circle lines, blue trilateral lines, and magenta square lines, respectively. The corresponding colored curves represent the theoretical predictions derived from Eq. 20. Additional parameters include $\beta = 0.5$ and $\mu = 0.5$ in the physical-contact layer, $\lambda = 0.15$, $\sigma_0 = 0.5$, and $\delta = 0.6$ in the virtual-contact layer.

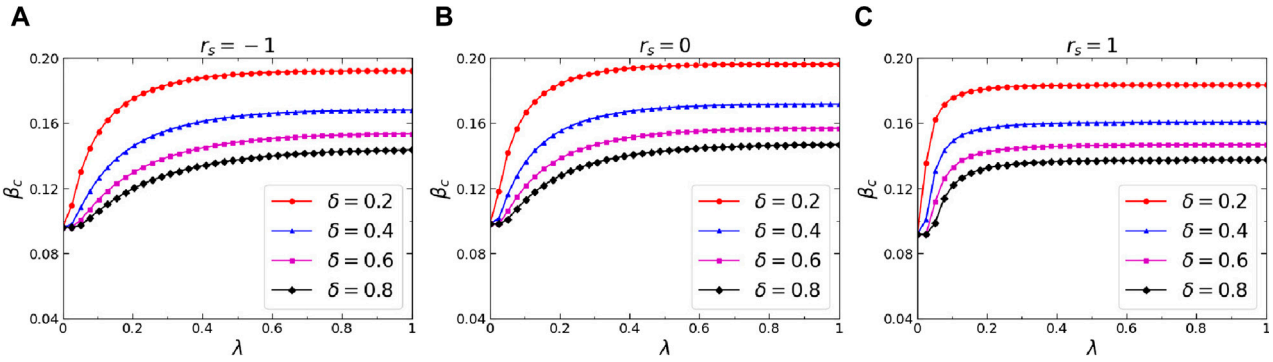

FIGURE 8
(Color online) Effects of the awareness forgetting probability δ on the epidemic threshold β_c. Specifically, the epidemic threshold β_c versus diffusion probability of awareness λ when **(A)** $r_s = -1$, **(B)** $r_s = 0$, and **(C)** $r_s = 1$. The results when $\delta = 0.2$, $\delta = 0.4$, $\delta = 0.6$, and $\delta = 0.8$ are denoted by red circle lines, blue trilateral lines, magenta square lines, and black rhombus lines, respectively. The corresponding colored curves represent the theoretical predictions derived from Eq. 20. Additional parameters include $\beta = 0.5$, $\gamma = 0$, and $\mu = 0.8$ in the physical-contact layer, $\sigma_0 = 0.5$ in the virtual-contact layer.

phenomenon can be explained by the fact that a higher average degree K_A in virtual-contact network facilitates the diffusion of awareness within the networks, resulting in a stronger inhibition on epidemic transmitting, thus β_c increases and λ_c decreases. To explore the influence of K_B on the epidemic threshold, we construct three multiplex networks G^{K_B-5}, G^{K_B-10}, and G^{K_B-30}, by randomly adding edges in the physical-contact layer of G^1. The values of K_B are configured as 5, 10, and 60, respectively, while maintaining a constant value of K_A at 10. Figures 9D–F show the changes of β_c concerning the diffusion probability of awareness λ on three multiplex networks under different combinations of awareness forgetting probability δ and infected individual recovery probability μ. Comparing the results from the figures, it can be concluded that on all the networks studied, an increase in K_B leads to a decrease in β_c when λ is constant. However, the change of K_B does not affect the metacritical point λ_c.

It should be noted that all the aforementioned results are based on the configured multiplex networks. To closely align with real-world scenarios, we conduct extensive experiments on a large number of real networks. The conclusions drawn from these experiments align with those from the configured multiplex networks. For a comprehensive overview of the detailed results, please refer to the Supplementary Material.

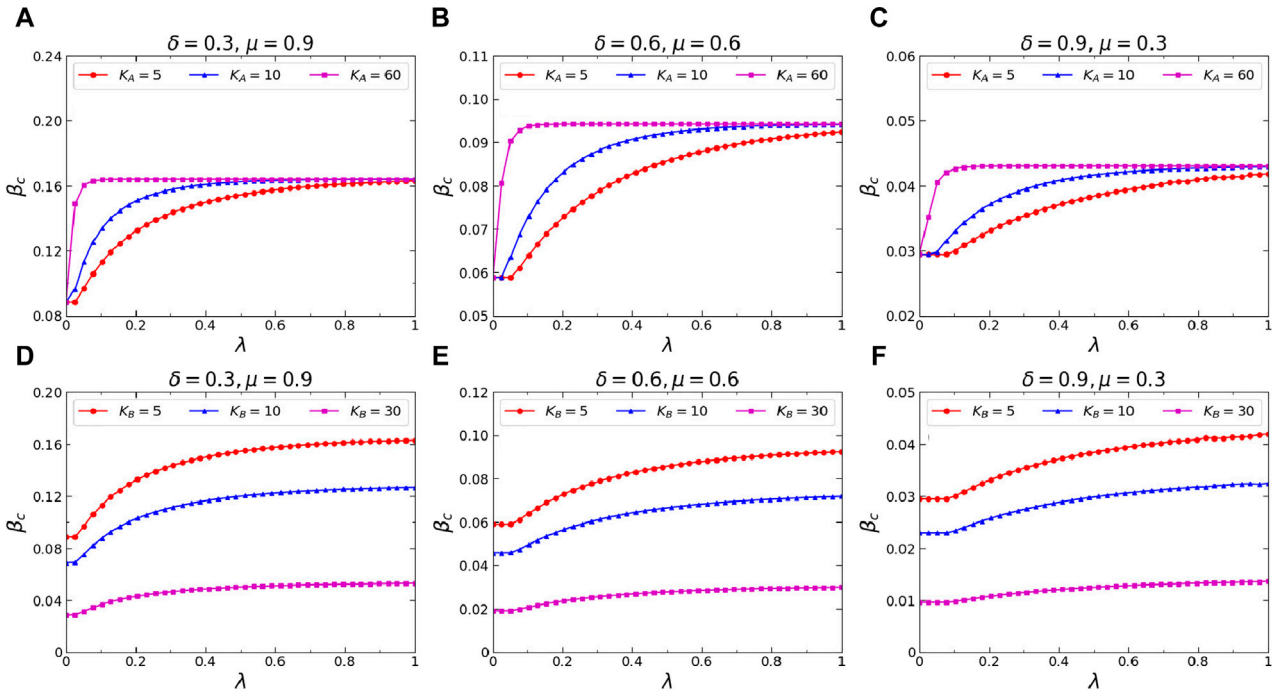

FIGURE 9
(Color online) Effects of the average degrees K_A and K_B of virtual-contact network and physical-contact network on the epidemic threshold β_c. Top: the epidemic threshold β_c versus awareness diffusion probability λ under different combinations of awareness forgetting probability δ and infected individual recovery probability, specifically, **(A)** $\delta = 0.3$, $\mu = 0.9$; **(B)** $\delta = 0.6$, $\mu = 0.6$; and **(C)** $\delta = 0.9$, $\mu = 0.3$. The results when $K_A = 5$, $K_A = 10$, and $K_A = 6$ are denoted by red circle lines, blue trilateral lines, and magenta square lines, respectively. Bottom: the epidemic threshold β_c versus diffusion probability of awareness λ when **(D)** $\delta = 0.3$, $\mu = 0.9$; **(E)** $\delta = 0.6$, $\mu = 0.6$; and **(F)** $\delta = 0.9$, $\mu = 0.3$. The results when $K_B = 5$, $K_B = 10$, and $K_B = 30$ are denoted by red circle lines, blue trilateral lines, and magenta square lines, respectively. The corresponding colored curves represent the theoretical predictions derived from Eq. 20. Additional parameters include $\beta = 0.5$ and $\gamma = 0.4$ in the physical-contact layer, $\sigma_0 = 0.5$, and $\lambda = 0.15$ in the virtual-contact layer.

5 Conclusion

The outbreak of an epidemic often stimulates the development of public awareness about disease prevention, which can effectively curb the process of epidemic transmission. Individuals generate different awareness responses due to varying amounts of information received from their neighbors. Therefore, considering the diversity in individual awareness responses is of significant research importance in the coupled awareness-epidemic dynamics. In this study, we first introduce a coupled awareness-epidemic dynamics model that incorporates the differences in individual awareness responses, where the self-initiated awareness probability of individuals is influenced by the number of their aware neighbors. Subsequently, we develop MMCA method for the analysis of the aforementioned model and validate the accuracy of the MMCA method in solving the coupled spreading model through MC numerical simulations. Next, we analyze the impact of crucial dynamics and structural parameters on the proposed coupled awareness-epidemic dynamics. Through abundant simulations and meticulous theoretical analyses, it has been demonstrated that individual awareness awakening can elevate the steady-state proportion of aware individuals on the networks, consequently mitigating epidemic transmission. Simultaneously, the impact of awareness diffusion on epidemic transmission exhibits a metacritical point λ_c. Specifically, when the awareness diffusion probability λ is larger than λ_c, the epidemic threshold β_c increases while the λ increases. Furthermore, the increase in the average degree K_A of the virtual-contact networks reduces the value of λ_c, while the change in the average degree K_B of the physical-contact networks do not affect λ_c. Finally, we conduct extensive experiments on a large number of real networks, yielding conclusions consistent with the configured multiplex networks. To sum up, this research comprehensively investigated the coupled awareness-epidemic dynamics with individualized self-initiated awareness. The research findings contribute to a deeper understanding of the interaction between awareness diffusion and epidemic transmission, providing essential theoretical insights for epidemic prevention and control.

Data availability statement

The datasets presented in this study are available upon request in the following online repository: https://github.com/20zyli3/zzz.

Author contributions

WZ: Methodology, Validation, Writing–original draft. YY: Methodology, Validation, Writing–original draft. ZL: Methodology, Validation, Writing–original draft. JX: Conceptualization, Funding acquisition, Methodology, Project administration, Software, Validation, Writing–original draft. TW: Methodology, Supervision, Validation, Writing–review and editing. DL: Supervision, Writing–review and editing. DH: Methodology,

Validation, Writing–original draft. ML: Methodology, Funding acquisition, Supervision, Writing–review and editing.

Funding

The author(s) declare that financial support was received for the research, authorship, and/or publication of this article. This work was supported by Shantou University under grants NTF20026 and NTF21041, the National Key Research and Development Program under Grant 2022YFB3104600, the China Postdoctoral Science Foundation Funded Project (2023M740519), Medico-Engineering Cooperation Funds from University of Electronic Science and Technology of China (Nos ZYGX2021YGLH213, ZYGX2022YGRH016), Interdisciplinary Crossing and Integration of Medicine and Engineering for Talent Training Fund, West China Hospital, Sichuan University under Grant No. HXDZ22010, the Municipal Government of Quzhou (Grant 2022D018, Grant 2022D029, Grant 2023D007, Grant 2023D015, Grant 2023D033, Grant 2023D034, Grant 2023D035), Zhejiang Provincial Natural Science Foundation of China under Grant No. LGF22G010009, and Guiding project of Quzhou Science and Technology Bureau (subject No 2022005, 2022K50, 2023K013, 2023K016).

Conflict of interest

The authors declare that the research was conducted in the absence of any commercial or financial relationships that could be construed as a potential conflict of interest.

Publisher's note

All claims expressed in this article are solely those of the authors and do not necessarily represent those of their affiliated organizations, or those of the publisher, the editors and the reviewers. Any product that may be evaluated in this article, or claim that may be made by its manufacturer, is not guaranteed or endorsed by the publisher.

Supplementary material

The Supplementary Material for this article can be found online at: https://www.frontiersin.org/articles/10.3389/fphy.2024.1437341/full#supplementary-material

References

1. Morens DM, Folkers GK, Fauci AS. The challenge of emerging and re-merging infectious diseases. *Nature* (2004) 430:242–9. doi:10.1038/nature02759

2. Shereen MA, Khan S, Kazmi A, Bashir N, Siddique R. Covid-19 infection: emergence, transmission, and characteristics of human coronaviruses. *J Adv Res* (2020) 24:91–8. doi:10.1016/j.jare.2020.03.005

3. Tangcharoensathien V, Calleja N, Nguyen T, Purnat T, D'Agostino M, Garcia-Saiso S, et al. Framework for managing the covid-19 infodemic: methods and results of an online, crowdsourced who technical consultation. *J Med Internet Res* (2020) 22:e19659. doi:10.2196/19659

4. Cirrincione L, Plescia F, Ledda C, Rapisarda V, Martorana D, Lacca G, et al. Covid-19 pandemic: new prevention and protection measures. *Sustainability* (2022) 14:4766. doi:10.3390/su14084766

5. Wu J, Zuo R, He C, Xiong H, Zhao K, Hu Z. The effect of information literacy heterogeneity on epidemic spreading in information and epidemic coupled multiplex networks. *Physica A: Stat Mech its Appl* (2022) 596:127119. doi:10.1016/j.physa.2022.127119

6. W X, C Z. Epidemic spreading with an awareness-based adaptive mechanism in temporal multiplex networks. *Front Phys* (2023) 11:1285480. doi:10.3389/fphy.2023.1285480

7. Ma W, Zhang P, Zhao X, Xue L. The coupled dynamics of information dissemination and seir-based epidemic spreading in multiplex networks. *Physica A: Stat Mech its Appl* (2022) 588:126558. doi:10.1016/j.physa.2021.126558

8. Liang GCX, Cui X, Zhu P. An effective method for epidemic suppression by edge removing in complex network. *Front Phys* (2023) 11:1164847. doi:10.3389/fphy.2023.1164847

9. Wang JW, Zhang HF, Ma XJ, Wang J, Ma C, Zhu PC. Privacy-preserving identification of the influential nodes in networks. *Int J Mod Phys C* (2023) 34. doi:10.1142/S0129183123501280

10. Shi D, Shang F, Chen B, Expert P, Lü L, Stanley HE, et al. Local dominance unveils clusters in networks. *Commun Phys* (2024) 7:170. doi:10.1038/s42005-024-01635-4

11. Ji P, Ye J, Mu Y, Lin W, Tian Y, Hens C, et al. Signal propagation in complex networks. *Phys Rep* (2023) 1017:1–96. doi:10.1016/j.physrep.2023.03.005

12. Li R, Wang W, Di Z. Effects of human dynamics on epidemic spreading in côte d'ivoire. *Physica A: Stat Mech its Appl* (2017) 467:30–40. doi:10.1016/j.physa.2016.09.059

13. Xiong X, Zeng Z, Feng M, Szolnoki A. Coevolution of relationship and interaction in cooperative dynamical multiplex networks. *Chaos: An Interdiscip J Nonlinear Sci* (2024) 34:023118. doi:10.1063/5.0188168

14. Lima CMAO. Information about the new coronavirus disease (covid-19). *Radiologia Brasileira* (2020) 53(2). doi:10.1590/0100-3984.2020.53.2e1

15. Deng G, Peng Y, Tian Y, Zhu X. Analysis of influence of behavioral adoption threshold diversity on multi-layer network. *Entropy* (2023) 25:458. doi:10.3390/e25030458

16. Tian Y, Tian H, Cui Q, Zhu X. Phase transition phenomena in social propagation with dynamic fashion tendency and individual contact. *Chaos: Solitons Fractals* (2024) 178:114366. doi:10.1016/j.chaos.2023.114366

17. Chen J, Liu Y, Yue J, Duan X, Tang M. Coevolving spreading dynamics of negative information and epidemic on multiplex networks. *Nonlinear Dyn* (2022) 110:3881–91. doi:10.1007/s11071-022-07776-x

18. Zhu X, Zhang J, Liu S, Tian Y, Cui Y, Li Y, et al. Behavioral propagation influenced by fluctuating personality on single-layer limited-contact network. *Physica Scripta* (2024) 99:025252. doi:10.1088/1402-4896/ad1960

19. Wang J, Cai S, Wang W, Zhou T. Link cooperation effect of cooperative epidemics on complex networks. *Appl Mathematics Comput* (2023) 437:127537. doi:10.1016/j.amc.2022.127537

20. Chen J, Liu Y, Tang M, Yue J. Asymmetrically interacting dynamics with mutual confirmation from multi-source on multiplex networks. *Inf Sci* (2022) 619:478–90. doi:10.1016/j.ins.2022.11.033

21. Chen Y, Liu Y, Tang M, Lai YC. Epidemic dynamics with non-markovian travel in multilayer networks. *Commun Phys* (2023) 6:263. doi:10.1038/s42005-023-01369-9

22. Cai SM, Chen XH, Ye XJ, Tang M. Precisely identifying the epidemic thresholds in real networks via asynchronous updating. *Appl Mathematics Comput* (2019) 361:377–88. doi:10.1016/j.amc.2019.05.039

23. Liu Y, Zeng Q, Pan L, Tang M. Identify influential spreaders in asymmetrically interacting multiplex networks. *IEEE Trans Netw Sci Eng* (2023) 10:2201–11. doi:10.1109/TNSE.2023.3243560

24. Wang J, Yang C, Chen B. The interplay between disease spreading and awareness diffusion in multiplex networks with activity-driven structure. *Chaos: An Interdiscip J Nonlinear Sci* (2022) 32:073104. doi:10.1063/5.0087404

25. Tian Y, Tian H, Cui Y, Zhu X, Cui Q. Influence of behavioral adoption preference based on heterogeneous population on multiple weighted networks. *Appl Mathematics Comput* (2023) 446:127880. doi:10.1016/j.amc.2023.127880

26. Wang J, Xiong W, Wang R, Cai S, Wu D, Wang W, et al. Effects of the information-driven awareness on epidemic spreading on multiplex networks. *Chaos: An Interdiscip J Nonlinear Sci* (2022) 32:073123. doi:10.1063/5.0092031

27. Wang R, Zhang X, Wang M. A two-layer model with partial mapping: unveiling the interplay between information dissemination and disease diffusion. *Appl Mathematics Comput* (2024) 468:128507. doi:10.1016/j.amc.2023.128507

28. Zhu P, Zhi Q, Guo Y, Wang Z. Analysis of epidemic spreading process in adaptive networks. *IEEE Trans Circuits Syst Express Briefs* (2018): 1252–6. doi:10.1109/TCSII.2018.2877406

29. Cao LWX, Zhao H, X A, An X. Competitive information propagation considering local-global prevalence on multi-layer interconnected networks. *Front Phys* (2023) 11:1293177. doi:10.3389/fphy.2023.1293177

30. Zhu P, Wang X, Li S, Guo Y, Wang Z. Investigation of epidemic spreading process on multiplex networks by incorporating fatal properties. *Appl Mathematics Comput* (2019) 359:512–24. doi:10.1016/j.amc.2019.02.049

31. Wang Z, Guo Q, Sun S, Xia C. The impact of awareness diffusion on sir-like epidemics in multiplex networks. *Appl Mathematics Comput* (2019) 349:134–47. doi:10.1016/j.amc.2018.12.045

32. Granell C, Gómez S, Arenas A. Dynamical interplay between awareness and epidemic spreading in multiplex networks. *Phys Rev Lett* (2013) 111:128701. doi:10.1103/PhysRevLett.111.128701

33. Granell C, G´omez S, Arenas A. Competing spreading processes on multiplex networks: awareness and epidemics. *Phys Rev E* (2014) 90:012808. doi:10.1103/PhysRevE.90.012808

34. Chen X, Gong K, Wang R, Cai S, Wang W. Effects of heterogeneous self-protection awareness on resource-epidemic coevolution dynamics. *Appl Mathematics Comput* (2020) 385:125428. doi:10.1016/j.amc.2020.125428

35. Wu D, Liu Y, Tang M, Xu XK, Guan S. Impact of hopping characteristics of inter-layer commuters on epidemic spreading in multilayer networks. *Chaos: Solitons and Fractals* (2022) 159:112100. doi:10.1016/j.chaos.2022.112100

36. Liu C, Yang Y, Chen B, Cui T, Shang F, Fan J, et al. Revealing spatiotemporal interaction patterns behind complex cities. *Chaos: An Interdiscip J Nonlinear Sci* (2022) 32:081105. doi:10.1063/5.0098132

37. Li C, Yuan Z, Li X. Epidemic threshold in temporal multiplex networks with individual layer preference. *IEEE Trans Netw Sci Eng* (2021):1. doi:10.1109/TNSE.2021.3055352